Astaxanthin suppresses lipopolysaccharide-induced myocardial injury by regulating MAPK and PI3K/AKT/mTOR/GSK3β signaling

WEN-JIE XIE[1*], GUO HOU[1*], LU WANG[1], SHA-SHA WANG[1] and XIAO-XING XIONG[2]

[1]Department of Critical Care Medicine; [2]Central Laboratory,
Renmin Hospital of Wuhan University, Wuhan, Hubei 430060, P.R. China

Received August 6, 2019; Accepted April 16, 2020

DOI: 10.3892/mmr.2020.11443

Abstract. Cardiac dysfunction is a significant manifestation of sepsis and it is associated with the prognosis of the disease. Astaxanthin (ATX) has been discovered to serve a variety of pharmacological effects, including anti-inflammatory, antioxidant and antiapoptotic properties. The present study aimed to investigate the role and mechanisms of ATX in sepsis-induced myocardial injury. Male C57BL/6 mice were divided into three groups (15 mice per group): Control group, lipopolysaccharide (LPS) group and LPS + ATX group. The cardiac dysfunction model was induced through an intraperitoneal injection of LPS (10 mg/kg) and ATX (40 mg/kg) was administered to the LPS + ATX group by intraperitoneal injection 30 min following the administration of LPS. All animals were sacrificed after 24 h. Inflammatory cytokine levels in the serum were detected using ELISAs, and cardiac B-type natriuretic peptide (BNP) levels were analyzed using western blot analysis and reverse transcription-quantitative PCR. Furthermore, the extent of myocardial injury was evaluated using pathological analysis, and cardiomyocyte apoptosis was analyzed using a TUNEL assay, in addition to determining the expression levels of Bcl-2 and Bax. The expression levels of proteins involved in the mitogen activated protein kinase (MAPK) and PI3K/AKT signaling pathways were also analyzed using western blot analysis. ATX significantly suppressed the LPS-induced increased production of TNF-α and IL-6 and suppressed the protein expression levels of BNP, Bax and Bcl-2 to normal levels. ATX also prevented the histopathological changes to the myocardial tissue and reduced the extent of necrosis. Furthermore, the treatment with ATX suppressed the LPS-activated MAPK and PI3K/AKT signaling. ATX additionally exerted a protective effect on cardiac dysfunction caused by sepsis by inhibiting MAPK and PI3K/AKT signaling.

Correspondence to: Dr Xiao-Xing Xiong, Central Laboratory, Renmin Hospital of Wuhan University, 238 Jiefang Road, Wuhan, Hubei 430060, P.R. China
E-mail: xiaoxingxiong@whu.edu.cn

*Contributed equally

Key words: astaxanthin, sepsis, cardiac dysfunction, inflammation, apoptosis

Introduction

Sepsis is a life-threatening organ dysfunction caused by a complex host response to an infection, and the hospital mortality rate of septic shock was >40% in 2016, worldwide (1). Cardiac dysfunction is a series complication of sepsis and it is associated with the prognosis of patients (2). Lipopolysaccharide (LPS) is a principal component of the cell wall in Gram-negative bacteria and it can trigger an inflammatory cascade reaction, which results in the synthesis and release of inflammatory mediators, such as tumor necrosis factor (TNF)-α, interleukin (IL)-1β and IL-6 (3). The overexpression of inflammatory factors could lead to endothelial injury and the disruption of vascular homeostasis, which could subsequently promote irreversible cardiac dysfunction (4). Therefore, the effective treatment of septic cardiac dysfunction may be beneficial for improving the prognosis of patients.

Astaxanthin (ATX) is a major carotenoid in marine organisms, which is ubiquitously present in the biological world, particularly in the feathers of shrimp, crab, fish, algae, yeast and birds (5). Previous studies have demonstrated that ATX serves a variety of beneficial physiological effects, including antioxidative, anti-inflammatory and antiapoptotic functions (6,7). In addition, it has been suggested that ATX may reduce the myocardial infarct area and improve the myocardial mitochondrial membrane potential and contractility index (7). Notably, it has also been reported that ATX may also protect against LPS-induced cardiac dysfunction by reducing the levels of inflammatory mediators and oxidative stress (8). However, the specific mechanisms by which ATX protects against LPS-induced cardiac dysfunction remain poorly understood.

The PI3K/AKT signaling pathway is involved in cell proliferation, differentiation and apoptosis (9), and it was revealed to serve an important role in cardiac dysfunction caused by sepsis (10). In a previous study, the mitogen activated protein kinase (MAPK) signaling pathway was also observed to

participate in the regulation of cell growth and differentiation, in addition to modulating the cell's response to cytokines and various stresses, such as TNF-α and LPS (11). Numerous studies have revealed that MAPK served a major role in promoting the production of inflammatory cytokines during sepsis, such as TNF-α, IL-6 (12,13). To investigate whether ATX exhibited protective effects during cardiac dysfunction the present study established an *in vivo* LPS-induced sepsis model using C57BL/6 mice to identify the possible underlying mechanisms of action of ATX. We hypothesized that ATX may be used for the treatment of LPS-induced cardiac dysfunction through the regulation of the PI3K/AKT and the MAPK signaling pathways. Understanding the mechanisms underlying the action of ATX may assist in the development of a novel treatment for patients with septic cardiomyopathy to improve the prognosis of patients.

Materials and methods

Animal studies. A total of 45 specific pathogen-free male C57BL/6 mice (age, 8-10 weeks; weight, 24-26 g) were obtained from The Institute of Laboratory of Animal Sciences, Chinese Academy of Medical Sciences and Peking Union Medical College. Mice were randomly divided into three groups (n=15 per group): Control, LPS and LPS + ATX. Animals were housed at a controlled temperature of 25˚C and a humidity of 45-50%, with a 12-h light/dark cycle and free access to standard laboratory water and chow; the animals were allowed to adapt to the laboratory conditions for 7 days prior to use for subsequent experiments. The animal experiments were approved by the Ethics Committee of Renmin Hospital of Wuhan University (Wuhan, China).

Induction of sepsis-associated cardiac dysfunction models. Cardiac dysfunction was induced by an intraperitoneal injection of LPS (10 mg/kg; cat. no. L2880; Sigma-Aldrich; Merck KGaA) for 24 h, as previously described (14). ATX (40 mg/kg; cat. no. SML0982; Sigma-Aldrich; Merck KGaA) dissolved in polyethylene glycol 400-N, N-dimethylacetamide (PEG400; 1:1 v/v; cat. no. 91863; Sigma-Aldrich; Merck KGaA) was administered to the mice in the LPS + ATX group 30 min after LPS administration for 24 h. The mice in the control and LPS groups were administered an equivalent volume of the vehicle (PEG400; 1:1 v/v; cat. no. 91863; Sigma-Aldrich; Merck KGaA). The health, behavior and death of mice were monitored every 6 h following LPS administration. In the LPS and LPS + ATX groups, 8 and 3 mice died, respectively, of severe infection following LPS treatment. All the surviving animals were anesthetized with pentobarbital solution (50 mg/kg) via an intraperitoneal injection 24 h after LPS treatment. Following anesthesia, 0.5 ml blood was collected from the mice by eyeball enucleation; which prompted two mice to die from severe anemia. To isolate myocardial tissue, mice were sacrificed by cervical dislocation. Following a 2 min observation, no respiration and corneal reflex in the mice confirmed death. The heart tissue was isolated post-mortem and stored in 4% paraformaldehyde or at -80˚C.

Mortality observation. The point at which LPS was administered was considered as the 0 h time point. The number of surviving mice was observed at 6, 12, 18 and 24 h after LPS injection and the mortality of each group was calculated using the following method: Mortality=dead mice/total number of mice x100%.

Analysis of blood samples using ELISA. Blood samples from the mice were collected from the posterior orbital plexus venous and were centrifuged at 4,200 x g for 10 min at room temperature. The supernatants were subsequently collected and stored at -20˚C. ELISA kits (cat. nos. EL-M0049c and E-EL-M0044c; Elabscience Biotechnology Co., Ltd.) were used to analyze the levels of TNF-α and IL-6 in the blood samples using an enzyme-labeled instrument (Multiskan MK3; Thermo Fisher Scientific, Inc.), according to the manufacturer's protocols.

Histological examination. Left ventricular and whole heart tissues were collected and fixed for 48 h in 4% paraformaldehyde at 4˚C, embedded in paraffin and sliced into 4-μm thick sections. The tissue sections were subsequently stained with hematoxylin & eosin (H&E) for 70 min at room temperature. Stained sections were visualized using a light microscope, at X100 and X200 magnification.

Reverse transcription-quantitative (RT-q)PCR. mRNA expression levels of B-type natriuretic peptide (BNP) were analyzed using RT-qPCR. The fresh frozen tissue stored at -80˚C was weighed to 100 mg, following which 1 ml TRIzol® reagent (cat. no. 15596026; Invitrogen; Thermo Fisher Scientific, Inc.) was added, and the tissue ground into a slurry using a homogenizer, according to the manufacturer's protocol. Total RNA was reverse transcribed into cDNA using a HiScript RT reagent kit (cat. no. R101-01/02; Vazyme Biotech Co., Ltd.), using the following conditions: 25˚C for 5 min, 50˚C for 15 min, 85˚C for 5 min then 4˚C for 10 min. qPCR was subsequently performed using a SYBRGreen master mix (cat. no. Q111-02; Vazyme Biotech Co., Ltd.), according to the manufacturer's protocol, on a QuantStudio 6 Flex Real-Time PCR system (Applied Biosystems; Thermo Fisher Scientific, Inc.), using the following conditions 50˚C for 2 min, 95˚C for 10 min, then 40 cycles of 95˚C for 30 sec and 60˚C for 30 sec. The data was analyzed with the $2^{-\Delta\Delta Cq}$ method (15). The primer sequences and the amplicon sizes of the target genes are presented in Table I. β-actin was used as the endogenous loading control.

Western blot analysis. To assess the expression levels and activation state of proteins in the MAPK and PI3K/AKT signaling pathways, total protein was extracted from the cardiac tissues. Cardiac tissues were collected and homogenized with a homogenizer using radioimmunoprecipitation assay lysis buffer (cat. no. P0013B), containing phenylmethanesulfonyl fluoride (cat. no. ST506) and phosphoesterase inhibitors (cat. no. S1873) (all Beyotime Institute of Biotechnology). Total protein was quantified using a bicinchoninic acid kit (cat. no. P0010; Beyotime Institute of Biotechnology) and 40 μg protein/lane was separated using 10% SDS-PAGE. The separated proteins were subsequently transferred onto a PVDF membrane (cat. no. IPVH00010; EMD Millipore) and blocked using 5% skimmed milk in Tris buffered saline containing 0.1% Tween-20 (TBST) for 2 h at room temperature.

Table I. Primer sequences and the amplicon sizes of the target genes used for the reverse transcription-quantitative PCR.

Gene	Primer sequence (5'→3')	Size (bp)
β-actin	F: CACGATGGAGGGGCCGGACTCATC	240
	R: TAAAGACCTCTATGCCAACACAGT	
B-type natriuretic peptide	F: GAGGTCACTCCTATCCTCTGG	202
	R: GCCATTTCCTCCGACTTTTCTC	

F, forward; R, reverse.

The membranes were incubated overnight at 4˚C in TBST containing 1% skimmed milk with the following primary antibodies: Anti-p38 (1:1,000; cat. no. 8690; Cell Signaling Technology, Inc.), anti-phosphorylated (p)-p38 (1:1,000; cat. no. 9211; Cell Signaling Technology, Inc.), anti-ERK1/2 (1:1,000; cat. no. ab17942; Abcam), anti-p-ERK1/2 (1:2,000; cat. no. 4370S; Cell Signaling Technology, Inc.), anti-JNK (1:1,000; cat. no. 9252S; Cell Signaling Technology, Inc.), anti-p-JNK (1:1,000; cat. no. 9251S; Cell Signaling Technology, Inc.), anti-PI3K (1:1,000; cat. no. 4257S; Cell Signaling Technology, Inc.), anti-p-PI3K (1:1,000; cat. no. ab182651; Abcam), anti-AKT (1:1,000; cat. no. 4691S; Cell Signaling Technology, Inc.), anti-p-AKT (1:1,000; cat. no. 9271T; Cell Signaling Technology, Inc.), anti-mTOR (1:500; cat. no. ab87540; Abcam), anti-p-mTOR (1:1,000; cat. no. 5536T; Cell Signaling Technology, Inc.), anti-glycogen synthase kinase-3 (1:500; GSK3) β (cat. no. ab93926; Abcam), anti-p-GSK3β (1:500; cat. no. ab75745; Abcam), anti-Bax (1:1,000; cat. no. ab32503; Abcam), anti-Bcl-2 (1:800; cat. no. 26593-1-AP; ProteinTech Group, Inc.) and anti-GAPDH (1:1,000; cat. no. AB-P-R 001; Hangzhou Goodhere Biotech Co., Ltd.). Following the incubation with the primary antibodies, the membranes were incubated with the following secondary antibodies for 2 h at 37˚C: Horseradish peroxidase (HRP) conjugated AffiniPure goat anti-mouse IgG (dilution 1:50,000; cat. no. BA1051) and HRP conjugated AffiniPure goat anti-rabbit IgG (dilution 1:50,000; cat. no. BA1054) (both Boster Biological Technology Co., Ltd). The protein bands were visualized using an ECL kit (Pierce; Thermo Fisher Scientific, Inc.) and densitometry analysis was performed using Bandscan v5.0 software (Glyko Biomedical Ltd.). The protein expression levels were normalized to GAPDH and phosphorylated proteins were normalized to the respective total protein.

TUNEL staining. A TUNEL assay was used to assess cardiomyocyte apoptosis. Briefly, heart tissues were collected, fixed and embedded as aforementioned, then the paraffin-embedded tissues were cut into 4-μm thick sections placed flat in 42˚C water bath and incubated at 60˚C. The tissue sections were deparaffinized, rinsed with PBS and incubated with proteinase K (20 μg/ml; cat. no. 40308ES20; Yeasen Biotech Co., Ltd) for 20 min at room temperature. A total of 50 μl TUNEL reaction mixture was subsequently added to each sample and the slices were placed in a wet box for 60 min at 37˚C in the dark. Following the incubation, the slides were rinsed with PBS (pH 7.4) three times for 5 min each and the cell nuclei were stained with DAPI (10 μg/ml) for 5 min at room temperature in the dark, and then washed with PBS four times for 5 min each time. Antifade mounting medium (cat. no. 0100-01; Southern Biotechnology Associates, Inc.) was used for sealing. TUNEL-positive cells were observed using a fluorescence microscope with 22 fields of view and X200 magnification; the apoptotic cells in the tissue sections fluoresced red and the nuclei fluoresced blue. The number of apoptotic and total cells were counted and the percentage of apoptotic cells were calculated using the following equation: Apoptosis index=apoptotic cells/total cells x100%.

Statistical analysis. Data are presented as the mean ± SD. Statistical differences among multiple groups were determined using an one-way ANOVA, followed by Tukey's post-hoc test. Kaplan-Meier survival curves were used to plot the mortality rates of the three groups and the differences in the survival between the groups were compared using a log-rank test. The experiments were repeated three times. All data were analyzed using SPSS version 17.0 (SPSS, Inc.). $P<0.05$ was considered to indicate a statistically significant difference.

Results

ATX improves the survival rate in septic mice. In the LPS group, following 6, 12, 18 and 24 h of LPS treatment, the number of deaths was 1, 2, 2 and 3, respectively, whereas in the LPS + ATX group, the number of deaths was 0, 1, 1 and 1, following 6, 12, 18 and 24 h of LPS treatment, respectively. The Kaplan-Meier survival curves revealed that the 24 h mortality rate of septic mice, induced by LPS without ATX administration, was 53.3%; however, the 24 h mortality rate decreased to 20% when treated with ATX, and this difference was significant (χ^2=11.989; P=0.002; Fig. 1).

ATX alleviates the inflammatory response and downregulates the expression levels of BNP. H&E staining demonstrated that LPS caused cardiomyocyte necrosis (indicated by the red arrows) and neutrophil infiltration (indicated by the blue arrows) in the LPS only group, while ATX treatment attenuated the LPS-induced necrosis (indicated by the red arrows) and neutrophil granulocyte infiltration (indicated by the blue arrows) in the myocardium (Fig. 2A). LPS treatment also significantly increased the protein and mRNA expression levels of BNP and the protein expression levels of the inflammatory cytokines, TNF-α and IL-6, compared with that in the control group, whereas ATX treatment significantly reversed these changes (Fig. 2B-D).

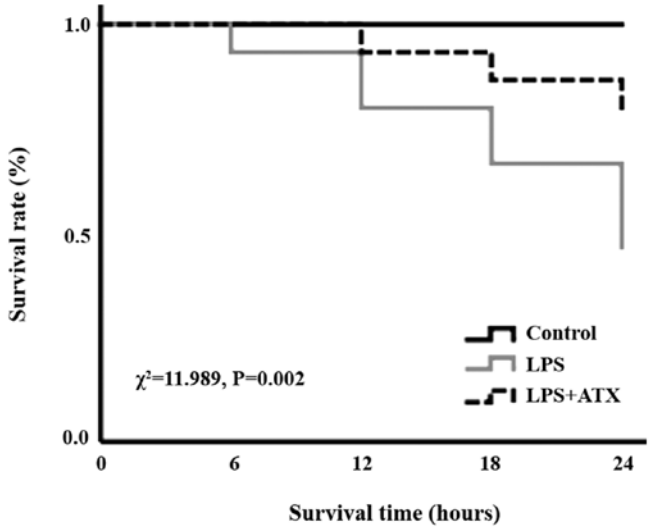

Figure 1. Effect of ATX on LPS-induced mouse mortality. Following 24 h of LPS treatment, the mortality rate in the LPS group was 53.3% and the mortality rate in the LPS + ATX group was 20%; this difference was significant (χ^2=11.989; P=0.002). ATX, astaxanthin; LPS, lipopolysaccharide.

ATX inhibits the levels of cardiomyocyte apoptosis in response to LPS. Compared with that in the control group, there was a marked increase in the levels of cardiomyocyte apoptosis in the LPS group; conversely, ATX treatment was observed to reduce the LPS-induced increased levels in cardiomyocyte apoptosis (Fig. 3A). Furthermore, LPS increased the protein expression levels of Bax and decreased the Bcl-2 protein expression levels in the LPS group, compared with that in the control group. ATX treatment decreased the protein expression levels of Bax and increased the Bcl-2 protein expression levels in the mice hearts following LPS treatment, compared with that in the LPS group (Fig. 3B and C).

ATX inhibits the activation of the MAPK signaling pathway. To investigate the anti-inflammatory molecular mechanisms of ATX, the activation state of proteins in the MAPK signaling pathway were analyzed. The administration of LPS was found to significantly increase the protein expression levels of p-p38, p-ERK and p-JNK compared with that in the control group (Fig. 4A and B); however, ATX treatment significantly decreased the LPS-induced expression levels of these proteins.

ATX inhibits the activation of the PI3K/AKT signaling pathway. To determine the mechanisms by which ATX reduced the apoptosis levels, the activation state of proteins in the PI3K/AKT signaling pathway was detected. The administration of LPS significantly increased the protein expression levels of p-PI3K, p-AKT, p-mTOR and p-GSK3β compared with that in the control group (Fig. 5A and B). In contrast, the treatment with ATX significantly reversed these trends observed in the LPS group (Fig. 5A and B).

Discussion

Sepsis is a significant public health concern and patients with septic shock had a high rate of mortality worldwide in 2016 (1). Septic shock frequently results in the dysfunction of multiple organs such as reduced hepatic clearance, elevated creatinine levels, and impaired aerobic respiration (1). The ventricular myocardium is depressed during sepsis and it has been discovered to exhibit features associated with diastolic dysfunction (16) and systolic dysfunction (17). Furthermore, the pathogenesis of septic cardiomyopathy has been associated with oxidative stress, increases in the production of inflammatory cytokines and apoptosis (17). However, the current therapeutic options available for cardiac dysfunction in sepsis are limited, and include hemofiltration techniques, statins, mesenchymal stem cells, and phosphodiesterase inhibitors (17). As a carotenoid, ATX has exhibited a variety of biological properties, including antioxidant, anti-inflammatory, antithrombotic and antiapoptotic functions (6,7).

LPS is highly pathogenic and can induce severe sepsis (18-21). In different studies, the mortality rate of mice was different following 24 h of intraperitoneal injection of LPS (10 mg/kg), such as 25, 36, 40 and 50% (18-21). In the present study, the mortality of mice after 24 h of LPS administration was 53.3%. As the principal component of the cell wall of Gram-negative bacteria, LPS can promote the synthesis and release of inflammatory mediators, such as TNF-α, IL-1β and IL-6 (3). Numerous studies have reported that proinflammatory mediators, including TNF-α, IL-1β and IL-6, were involved in the occurrence and development of myocardial dysfunction (4,22). For example, TNF-α was discovered to induce myocardial depression through the modulation of the inflammatory response (23,24). Furthermore TNF-α was identified to serve as a modulator of secondary factors (25), such as nitric oxide and caspase activation, which induced myocardial apoptosis leading to cardiac dysfunction (26). IL-6 is an important mediator of cardiac inflammation and dysfunction; in a previous study, IL-6 knockout mice were found to have a reduced inflammatory response and the levels of apoptosis, and an improved systolic function following sepsis, compared with that in the wild-type mice (27). The present study revealed that following 24 h of LPS administration, the levels of the inflammatory factors in the serum of mice were significantly increased, whereas ATX treatment decreased the synthesis and release of TNF-α and IL-6, and prevented LPS-induced cardiac function.

The MAPK signaling pathway serves an important role in inflammation and MAPKs were discovered to be important mediators that drive the production of inflammatory cytokines in sepsis (12). For example, the activation of p38 was observed to stimulate monocyte and macrophages to produce TNF-α and IL-6, while the inhibition of p38 exerted a significant protective effect on lung tissue and cardiomyocytes (28,29). In addition, the JNK signaling pathway was reported to serve an active role in the inflammatory response by promoting the release of TNF-α, IL-1β and IL-6 (30). The activation of inflammation requires two distinct steps: Priming and activation. The priming or licensing of the inflammasome are independent of transcription and translation, and they are centered upon the ERK signaling pathway (31). In a previous study using the standard model of LPS priming followed by ATP, an ERK inhibitor (U0126) was found to significantly block inflammasome priming and activation (31). However, the inhibition of ERK following priming was unable to block LPS/ATP-mediated human monocyte inflammasome

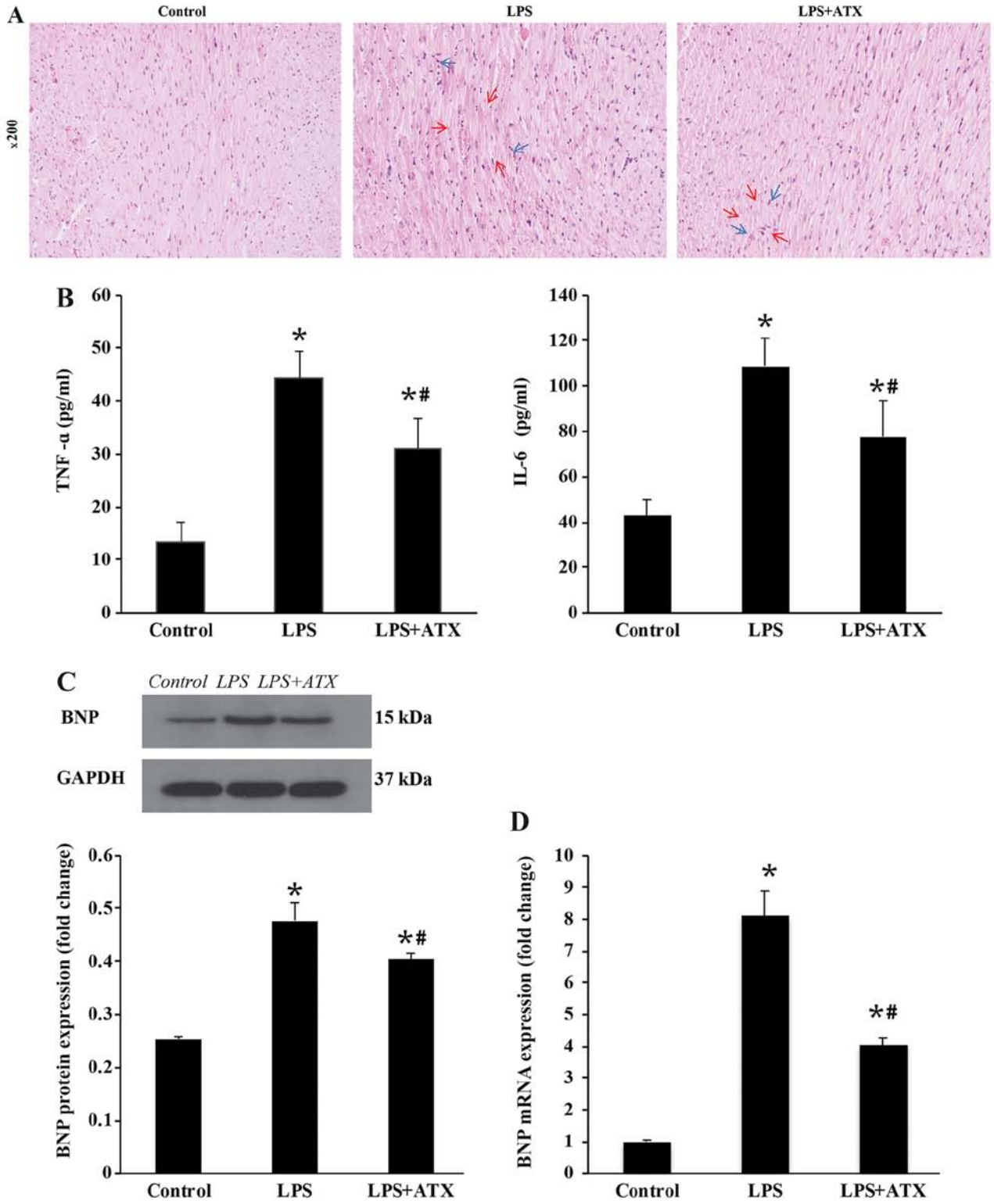

Figure 2. Effect of ATX on inflammation infiltration and BNP expression levels. (A) Hematoxylin & eosin staining demonstrated that ATX attenuated myocardial necrosis (indicated by the red arrows) and neutrophil infiltration (indicated by the blue arrows). (B) ELISAs were used to demonstrated that ATX treatment reduced the secreted levels of TNF-α and IL-6. (C) Protein expression levels of BNP were determined using western blot analysis. (D) Reverse transcription-quantitative PCR was used to analyze the mRNA expression levels of BNP. Data are presented as the mean ± SD from three independent experiments. *P<0.05 vs. control; #P<0.05 vs. LPS. ATX, Astaxanthin; LPS, lipopolysaccharide; TNF-α, tumor necrosis factor α; IL, interleukin; BNP, B-type natriuretic peptide.

activation (32). Consistent with the findings of the previous studies, the present study also demonstrated that ATX inhibited the production of inflammation by inhibiting the p38/JNK/ERK signaling pathway. PI3K/AKT signaling is also involved in the inflammatory response; for example, Stark *et al* (33) reported that PI3K/AKT signaling served a complex role in the coordination of both proinflammatory and anti-inflammatory pathways, which promoted the

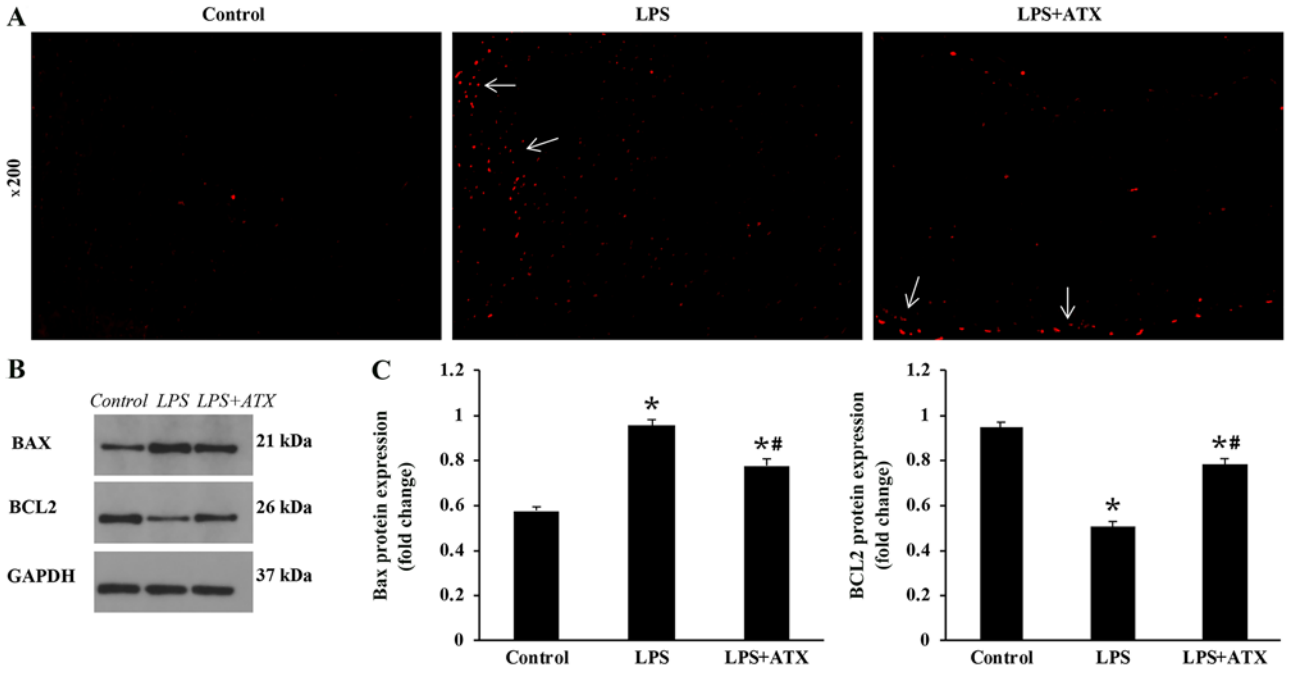

Figure 3. Effect of ATX on LPS-induced myocardial apoptosis. (A) TUNEL staining was used to reveal that ATX treatment alleviated the levels of cardiomyocyte apoptosis (red dots indicated by the white arrows). The protein expression levels of Bax and Bcl-2 were determined using (B) Western blot analysis and the results were subsequently (C) semi-quantified. Data are presented as the mean ± SD from three independent experiments. *P<0.05 vs. control; #P<0.05 vs. LPS. ATX, Astaxanthin; LPS, lipopolysaccharide.

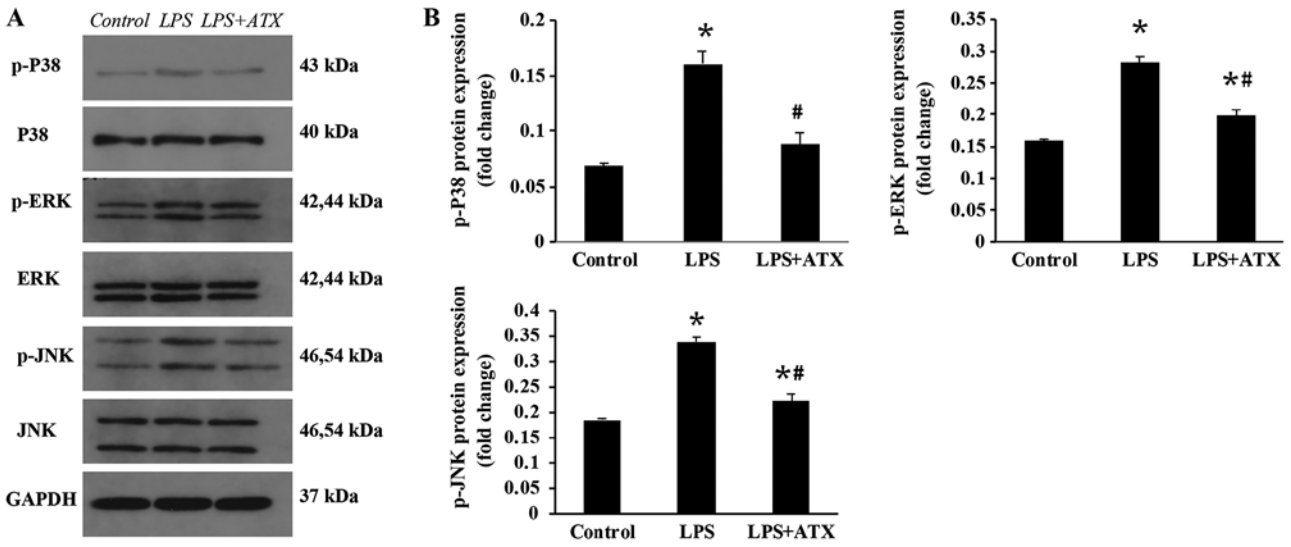

Figure 4. Inhibitory effects of ATX on the mitogen activated protein kinase signaling pathway. The protein expression levels of p-p38, p38, p-ERK, ERK, p-JNK and JNK was determined using (A) western blot analysis and the results were subsequently (B) semi-quantified. Data are presented as the mean ± SD from three independent experiments. *P<0.05 vs. control; #P<0.05 vs. LPS. ATX, Astaxanthin; LPS, lipopolysaccharide; p-, phosphorylated.

production of proinflammatory cytokines through NF-κB activation downstream of AKT, and exerted an inhibitory effect on toll-like receptor (TLR)2, TLR3 and TLR4-mediated inflammation through the AKT-dependent inhibition of GSK3β and forkhead box O1, respectively. Jope *et al* (34) also demonstrated that the activation of TLR4 induced the production of cytokines through myeloid differentiation factor 88 (MyD88)-dependent and MyD88-independent pathways, and GSK3 enhanced the inflammatory signaling via both pathways. In addition, numerous studies have reported that the TLR4/MAPK signaling pathway is an important mechanism of inflammatory activation in sepsis (35,36). Therefore, the PI3K/AKT pathway may also promote or inhibit the MAPK pathway, which stimulates the production of inflammatory factors, and ATX may mitigate the septic myocardial injury by partially blocking the activation of the MAPK and PI3K/AKT signaling pathways.

The PI3K/AKT signaling pathway serves an important role in cell proliferation, differentiation, apoptosis and survival (9). mTOR and GSK3β, downstream members of the

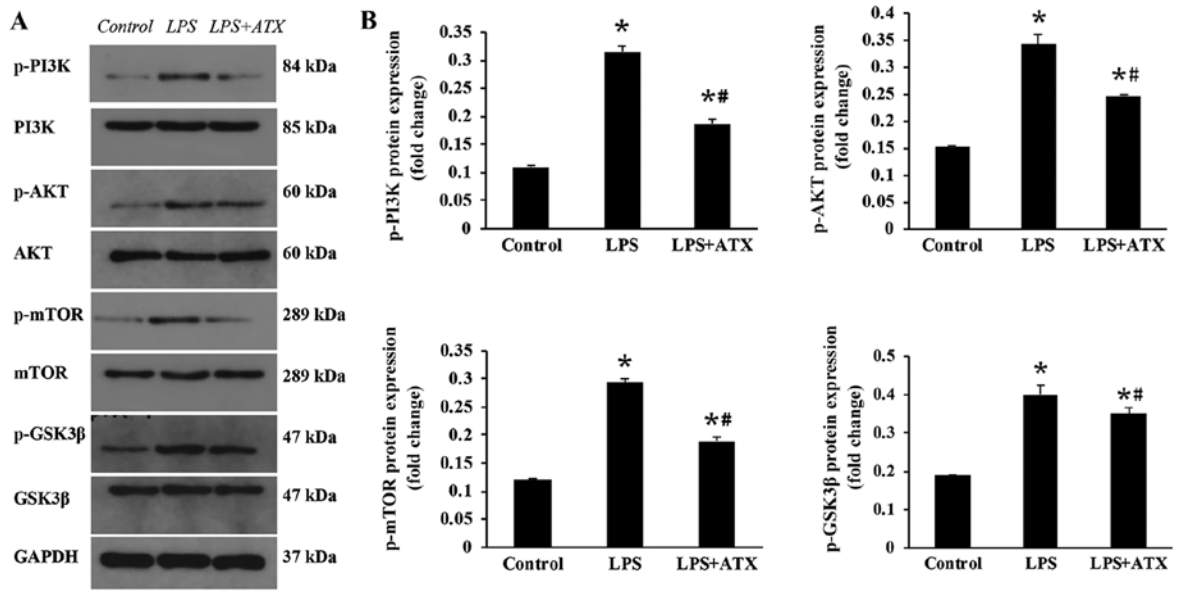

Figure 5. Effect of ATX on the PI3K/AKT signaling pathway. The protein expression levels of p-PI3K, PI3K, p-AKT, AKT, p-mTOR, mTOR, p-GSK3β and GSK3β were determined using (A) western blot analysis and the results were subsequently (B) semi-quantified. Data are presented as the mean ± SD from three independent experiments. *P<0.05 vs. control; #P<0.05 vs. LPS. ATX, Astaxanthin; LPS, lipopolysaccharide; GSK3β, glycogen synthase kinase-3β; p-, phosphorylated.

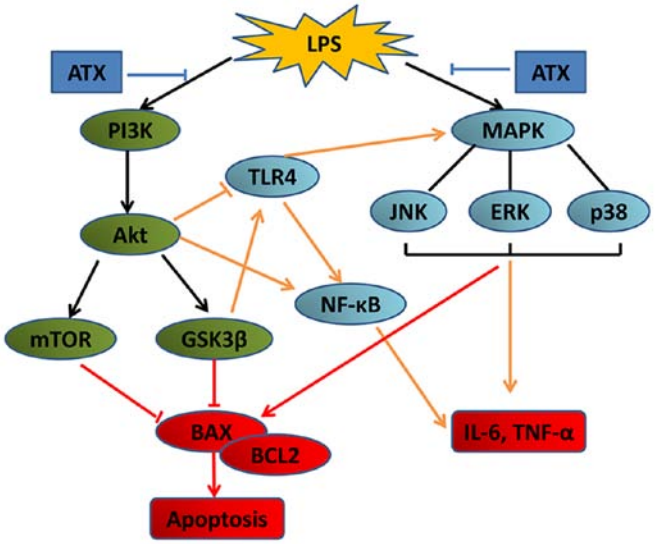

Figure 6. Schematic diagram of the potential mechanism by which ATX inhibits LPS-induced myocardial injury. ATX, Astaxanthin; LPS, lipopolysaccharide; GSK3β, glycogen synthase kinase-3β; TLR4, toll-like receptor 4; IL, interleukin; TNF-α, tumor necrosis factor-α.

AKT signaling pathway, were discovered to be involved in the regulation of cell apoptosis (37,38). The PI3K/AKT signaling pathway has also been associated with septic myocardial injury, and the inhibition of the PI3K/AKT signaling pathway was observed to mitigate myocardial injury in sepsis (10). In the present study, the protein expression levels of p-PI3K, p-AKT, p-mTOR and p-GSK3β were increased in the LPS-treated mice, whereas ATX reversed these increased expression levels of p-PI3K, p-AKT, p-mTOR and p-GSK3β, suggesting an anti-apoptotic effect. However, the PI3K/AKT signaling pathway is known to inhibit apoptosis (9). MAPK signaling is involved in apoptosis and JNK signaling was discovered to induce activator protein-1 dependent Bax and caspase activation, which resulted in neuronal apoptosis (39). In a review by Lu and Xu (40) the authors found that the activation of ERK1/2 typically promoted cell survival; however, under certain conditions, ERK1/2 exhibited proapoptotic functions. Therefore, sepsis-induced myocardial apoptosis may be associated with the p38/JNK/ERK signaling pathway. In addition, the reactivation of AKT, following hypoxia or ischemia, was revealed to be regulated by JNKs (41). Chaanine *et al* (42) discovered that both JNK and AKT activities increased with pressure overload; however, JNK signaling was dominant over AKT signaling for the activation of the transcription factor, FOXO3a and for the transcription of its effector, BNIP3, promoting mitochondrial apoptosis. Therefore, we hypothesized that both the MAPK and the PI3K/AKT signaling pathways were activated by LPS, and signaling via the MAPK pathway was more prominent compared with signaling via the PI3K/AKT pathway, which thus increased apoptosis. In the present study, ATX inhibited the activation of the MAPK and PI3K/AKT signaling pathways and reduced the protein expression levels of Bax/ Bcl-2, which protected the myocardium from apoptosis in sepsis.

At present, the most common methods for modeling sepsis include intraperitoneal injection or intravenous injection with LPS; however, cecal ligation and puncture have been found to improve the development of sepsis and clinical infection (43). This is achieved by necrotizing the end of the cecum following surgery and enabling the contents to enter the abdominal cavity following intestinal puncture; however, this method is affected by the bacterial composition of the intestinal contents and differences between operators (44). The model of sepsis induced with LPS by tail vein injection is acute, and acute cardiac dysfunction can be induced within 4-6 h (45). LPS can also be injected intraperitoneally to induce septic myocardial injury after 6 h; the dosage of LPS is easy to control and the surgery is simple; however, the model of LPS administration

does not reflect all the complex physiological human responses, such as proinflammatory cytokines production, hemodynamic response (46,47). A previous study used PEG400 as an ATX solvent and confirmed that PEG400 exerted no significant effect on the experiment (48). Thus, ATX dissolved in PEG400 was administered to the mice in the LPS + ATX group in the present study.

Nonetheless, the results of the current study are limited. BNP is an important indicator of cardiac dysfunction, which has been discovered to be significantly associated with sepsis induced myocardial dysfunction and mortality in patients with septic shock (49). Thus, due to the limited conditions in the present study, only BNP was selected to evaluate cardiac function without ultrasonic, hemodynamic and electrocardiography methods. Our future studies aim to improve the experimental method.

In conclusion, the present study demonstrated that compared with that in the LPS group, ATX treatment significantly reduced the levels of IL-6 and TNF-α in the serum, reversed the histopathological alterations and inhibited the LPS-induced apoptosis of mouse cardiomyocytes. Furthermore, the increased mRNA and protein expression levels of BNP induced by LPS were reversed by ATX, and ATX treatment reduced the mortality rates in mice with sepsis. Together, these data indicate that ATX may exhibit a protective effect on LPS-induced cardiac dysfunction in septic mice. Thus, ATX treatment may protect the heart from sepsis and lower the mortality rates in mice. The mechanisms of ATX may be related to the inhibition of the MAPK and PI3K/AKT/mTOR/GSK3β signaling pathways (Fig. 6). Therefore, ATX may serve as a potentially effective intervention for the treatment of cardiac dysfunction in patients with sepsis.

Acknowledgements

Not applicable.

Funding

This study was supported by the National Natural Science Foundation of China (grant nos. 81870939 and 81571147).

Availability of data and materials

The datasets used and/or analyzed during the current study are available from the corresponding author on reasonable request.

Authors' contributions

WJX and GH designed the experiments. LW and SSW performed the experiments. GH performed the statistical analysis. WJX prepared the manuscript. XXX designed the experiments, interpreted and analyzed the data, and revised the manuscript. All authors read and approved the final manuscript.

Ethics approval and consent to participate

All animal experiments were conducted in accordance with the institutional guidelines of the Animal Care and Use Committee of Renmin Hospital of Wuhan University (Wuhan, China).

Patient consent for publication

Not applicable.

Competing interests

The authors declare that they have no competing interests.

References

1. Singer M, Deutschman CS, Seymour CW, Shankar-Hari M, Annane D, Bauer M, Bellomo R, Bernard GR, Chiche JD, Coopersmith CM, *et al*: The third international consensus definitions for sepsis and septic shock (sepsis-3). JAMA 315: 801-810, 2016.
2. Merx MW and Weber C: Sepsis and the heart. Circulation 116: 793-802, 2007.
3. Matsuda N and Hattori Y: Systemic inflammatory response syndrome (SIRS): Molecular pathophysiology and gene therapy. J Pharmacol Sci 101: 189-198, 2006.
4. Siti HN, Kamisah Y and Kamsiah J: The role of oxidative stress, antioxidants and vascular inflammation in cardiovascular disease (a review). Vascul Pharmacol 71: 40-56, 2015.
5. Hussein G, Nakamura M, Zhao Q, Iguchi T, Goto H, Sankawa U and Watanabe H: Antihypertensive and neuroprotective effects of astaxanthin in experimental animals. Biol Pharm Bull 28: 47-52, 2005.
6. Wu H, Niu H, Shao A, Wu C, Dixon BJ, Zhang J, Yang S and Wang Y: Astaxanthin as a potential neuroprotective agent for neurological diseases. Mar Drugs 13: 5750-5766, 2015.
7. Fassett RG and Coombes JS: Astaxanthin: A potential therapeutic agent in cardiovascular disease. Mar Drugs 9: 447-465, 2011.
8. Zhou L, Gao M, Xiao Z, Zhang J, Li X and Wang A: Protective effect of astaxanthin against multiple organ injury in a rat model of sepsis. J Surg Res 195: 559-567, 2015.
9. Kandel ES and Hay N: The regulation and activities of the multifunctional serine/threonine kinase Akt/PKB. Exp Cell Res 253: 210-229, 1999.
10. Chen L, Liu P, Feng X and Ma C: Salidroside suppressing LPS-induced myocardial injury by inhibiting ROS-mediated PI3K/Akt/mTOR pathway in vitro and in vivo. J Cell Mol Med 21: 3178-3189, 2017.
11. Joh EH, Gu W and Kim DH: Echinocystic acid ameliorates lung inflammation in mice and alveolar macrophages by inhibiting the binding of LPS to TLR4 in NF-κB and MAPK pathways. Biochem Pharmacol 84: 331-340, 2012.
12. Frazier WJ, Wang X, Wancket LM, Li XA, Meng X, Nelin LD, Cato AC and Liu Y: Increased inflammation, impaired bacterial clearance, and metabolic disruption after gram-negative sepsis in Mkp-1-deficient mice. J Immunol 183: 7411-7419, 2009.
13. Wang X, Meng X, Kuhlman JR, Nelin LD, Nicol KK, English BK and Liu Y: Knockout of Mkp-1 enhances the host inflammatory responses to gram-positive bacteria. J Immunol 178: 5312-5320, 2007.
14. Lee SJ, Bai SK, Lee KS, Namkoong S, Na HJ, Ha KS, Han JA, Yim SV, Chang K, Kwon YG, *et al*: Astaxanthin inhibits nitric oxide production and inflammatory gene expression by suppressing I(kappa)B kinase-dependent NF-kappaB activation. Mol Cells 16: 97-105, 2003.
15. Livak KJ and Schmittgen TD: Analysis of relative gene expression data using real-time quantitative PCR and the 2(-Delta Delta C(T)) method. Methods 25: 402-408, 2001.
16. Kakihana Y, Ito T, Nakahara M, Yamaguchi K and Yasuda T: Sepsis-induced myocardial dysfunction: Pathophysiology and management. J Intensive Care 4: 22, 2016.
17. Balija TM and Lowry SF: Lipopolysaccharide and sepsis-associated myocardial dysfunction. Curr Opin Infect Dis 24: 248-253, 2011.
18. Honda T, He Q, Wang F and Redington AN: Acute and chronic remote ischemic conditioning attenuate septic cardiomyopathy, improve cardiac output, protect systemic organs, and improve mortality in a lipopolysaccharide-induced sepsis model. Basic Res Cardiol 114: 15, 2019.

19. de Pádua Lúcio K, Rabelo ACS, Araújo CM, Brandão GC, de Souza GHB, da Silva RG, de Souza DMS, Talvani A, Bezerra FS, Calsavara AJC and Costa DC: Anti-inflammatory and antioxidant properties of black mulberry (Morus nigra L.) in a model of LPS-induced sepsis. Oxid Med Cell Longev 2018: 5048031, 2018.
20. Kawaguchi S, Okada M, Ijiri E, Koga D, Watanabe T, Hayashi K, Kashiwagi Y, Fujita S and Hasebe N: β_3-Adrenergic receptor blockade reduces mortality in endotoxin-induced heart failure by suppressing induced nitric oxide synthase and saving cardiac metabolism. Am J Physiol Heart Circ Physiol 318: H283-H294, 2020.
21. Kumari A, Dash D and Singh R: Curcumin inhibits lipopolysaccharide (LPS)-induced endotoxemia and airway inflammation through modulation of sequential release of inflammatory mediators (TNF-α and TGF-β1) in murine model. Inflammopharmacology 25: 329-341, 2017.
22. Romero-Bermejo FJ, Ruiz-Bailen M, Gil-Cebrian J and Huertos-Ranchal MJ: Sepsis-induced cardiomyopathy. Curr Cardiol Rev 7: 163-183, 2011.
23. Kapadia S, Lee J, Torre-Amione G, Birdsall HH, Ma TS and Mann DL: Tumor necrosis factor-alpha gene and protein expression in adult feline myocardium after endotoxin administration. J Clin Invest 96: 1042-1052, 1995.
24. Haudek SB, Bryant DD and Giroir BP: Differential regulation of myocardial NF kappa B following acute or chronic TNF-alpha exposure. J Mol Cell Cardiol 33: 1263-1271, 2001.
25. Meldrum DR: Tumor necrosis factor in the heart. Am J Physiol 274: R577-R595, 1998.
26. Carlson DL, Willis MS, White DJ, Horton JW and Giroir BP: Tumor necrosis factor-alpha-induced caspase activation mediates endotoxin-related cardiac dysfunction. Crit Care Med 33: 1021-1028, 2005.
27. Zhang H, Wang HY, Bassel-Duby R, Maass DL, Johnston WE, Horton JW and Tao W: Role of interleukin-6 in cardiac inflammation and dysfunction after burn complicated by sepsis. Am J Physiol Heart Circ Physiol 292: H2408-H2416, 2007.
28. Nick JA, Young SK, Arndt PG, Lieber JG, Suratt BT, Poch KR, Avdi NJ, Malcolm KC, Taube C, Henson PM and Worthen GS: Selective suppression of neutrophil accumulation in ongoing pulmonary inflammation by systemic inhibition of p38 mitogen-activated protein kinase. J Immunol 169: 5260-5269, 2002.
29. Frazier WJ, Xue J, Luce WA and Liu Y: MAPK signaling drives inflammation in LPS-stimulated cardiomyocytes: The route of crosstalk to G-protein-coupled receptors. PLoS One 7: e50071, 2012.
30. Li ST, Dai Q, Zhang SX, Liu YJ, Yu QQ, Tan F, Lu SH, Wang Q, Chen JW, Huang HQ and Li M: Ulinastatin attenuates LPS-induced inflammation in mouse macrophage RAW264.7 cells by inhibiting the JNK/NF-κB signaling pathway and activating the PI3K/Akt/Nrf2 pathway. Acta Pharmacol Sin 39: 1294-1304, 2018.
31. Ghonime MG, Shamaa OR, Das S, Eldomany RA, Fernandes-Alnemri T, Alnemri ES, Gavrilin MA and Wewers MD: Inflammasome priming by lipopolysaccharide is dependent upon ERK signaling and proteasome function. J Immunol 192: 3881-3888, 2014.
32. Mehta VB, Hart J and Wewers MD: ATP-stimulated Release of interleukin (IL)-1beta and IL-18 requires priming by lipopolysaccharide and is independent of caspase-1 cleavage. J Biol Chem 276: 3820-3826, 2001.
33. Stark AK, Sriskantharajah S, Hessel EM and Okkenhaug K: PI3K inhibitors in inflammation, autoimmunity and cancer. Curr Opin Pharmacol 23: 82-91, 2015.
34. Jope RS, Cheng Y, Lowell JA, Worthen RJ, Sitbon YH and Beurel E: Stressed and inflamed, can gsk3 be blamed?. Trends Biochem Sci 42: 180-192, 2017.
35. Liu C, Tang X, Zhang W, Li G, Chen Y, Guo A and Hu C: 6-bromoindirubin-3'-oxime suppresses LPS-induced inflammation via inhibition of the TLR4/NF-κB and TLR4/MAPK signaling pathways. Inflammation 42: 2192-2204, 2019.
36. Park J, Ha SH, Abekura F, Lim H, Magae J, Ha KT, Chung TW, Chang YC, Lee YC, Chung E, *et al*: 4-O-carboxymethylascochlorin inhibits expression levels of on inflammation-related cytokines and matrix metalloproteinase-9 through NF-κB/MAPK/TLR4 signaling pathway in LPS-activated RAW264.7 cells. Front Pharmacol 10: 304, 2019.
37. Kumar D, Shankar S and Srivastava RK: Rottlerin induces autophagy and apoptosis in prostate cancer stem cells via PI3K/Akt/mTOR signaling pathway. Cancer Lett 343: 179-189, 2014.
38. Guo B, Zhang W, Xu S, Lou J, Wang S and Men X: GSK-3β mediates dexamethasone-induced pancreatic β cell apoptosis. Life Sci 144: 1-7, 2016.
39. Putcha GV, Le S, Frank S, Besirli CG, Clark K, Chu B, Alix S, Youle RJ, Lamarche A, Maroney AC and Johnson EM Jr: JNK-mediated BIM phosphorylation potentiates BAX-dependent apoptosis. Neuron 38: 899-914, 2003.
40. Lu Z and Xu S: ERK1/2 MAP kinases in cell survival and apoptosis. IUBMB Life 58: 621-631, 2006.
41. Shao Z, Bhattacharya K, Hsich E, Park L, Walters B, Germann U, Wang YM, Kyriakis J, Mohanlal R, Kuida K, *et al*: c-jun N-terminal kinases mediate reactivation of Akt and cardiomyocyte survival after hypoxic injury in vitro and in vivo. Circ Res 98: 111-118, 2005.
42. Chaanine AH, Jeong D, Liang L, Chemaly ER, Fish K, Gordon RE and Hajjar RJ: JNK modulates FOXO3a for the expression of the mitochondrial death and mitophagy marker BNIP3 in pathological hypertrophy and in heart failure. Cell Death Dis 3: 265, 2012.
43. Fink MP: Animal models of sepsis. Virulence 5: 143-153, 2014.
44. Hubbard WJ, Choudhry M, Schwacha MG, Kerby JD, Rue LW III, Bland KI and Chaudry IH: Cecal ligation and puncture. Shock 24 (Supp 1): S52-S57, 2005.
45. Wang X, Su L, Yang R, Zhang H and Liu D: Myocardial strain/stress changes identified by echocardiography may reveal early sepsis-induced myocardial dysfunction. J Int Med Res 46: 1439-1454, 2018.
46. Dejager L, Pinheiro I, Dejonckheere E and Libert C: Cecal ligation and puncture: The gold standard model for polymicrobial sepsis?. Trends Microbiol 19: 198-208, 2011.
47. Diao X and Sun S: PMicroRNA-124a regulates LPS-induced septic cardiac dysfunction by targeting STX2. Biotechnol Lett 39: 1335-1342, 2017.
48. Guo SX, Zhou HL, Huang CL, You CG, Fang Q, Wu P, Wang XG and Han CM: Astaxanthin attenuates early acute kidney injury following severe burns in rats by ameliorating oxidative stress and mitochondrial-related apoptosis. Marine Drugs 13: 2105-2123, 2015.
49. Kakoullis L, Giannopoulou E, Papachristodoulou E, Pantzaris ND, Karamouzos V, Kounis NG, Koniari I and Velissaris D: The utility of brain natriuretic peptides in septic shock as markers for mortality and cardiac dysfunction: A systematic review. Int J Clin Pract 73: e13374, 2019.